

General Disclaimer

One or more of the Following Statements may affect this Document

- This document has been reproduced from the best copy furnished by the organizational source. It is being released in the interest of making available as much information as possible.
- This document may contain data, which exceeds the sheet parameters. It was furnished in this condition by the organizational source and is the best copy available.
- This document may contain tone-on-tone or color graphs, charts and/or pictures, which have been reproduced in black and white.
- This document is paginated as submitted by the original source.
- Portions of this document are not fully legible due to the historical nature of some of the material. However, it is the best reproduction available from the original submission.

Are the Stratospheric Dust Particles Meteor Ablation Debris or Interplanetary Dust?

Maxwell B. Blanchard and Frank T. Kyte

(NASA-TM-78507) ARE THE STRATOSPHERIC DUST
PARTICLES METEOR ABLATION DEBRIS OR
INTERPLANETARY DUST? (NASA) 50 p HC A03/MF
A01 CACL 03B

N78-34014

Unclas
G3/90 33798

August 1978



NASA

National Aeronautics and
Space Administration

Are the Stratospheric Dust Particles Meteor
Ablation Debris or Interplanetary Dust?

Maxwell B. Blanchard and Frank T. Kyte¹

Ames Research Center, NASA


Moffett Field, California 94035

ABSTRACT

Recent collections of 5 - 50 micron particles from the stratosphere may soon be the object of intense research as a source of interplanetary dust that may provide information about the origin of the solar system. Before the interplanetary dust can be studied in depth, it is necessary to identify and separate the meteor ablation debris from the stratospheric collection. Criteria for recognizing meteor ablation debris was developed based on studies of natural and laboratory created fusion crusts and debris from artificial meteor samples. These laboratory studies indicate that meteor ablation debris from nickel-iron meteoroids produce spherules containing taenite, wüstite, magnetite, and hematite. These same studies also indicate that ablation debris from chondritic meteoroids produce spheres and fragmentary debris. The spheres may be either silicate rich, containing zoned olivine, magnetite, and glass, or sulfide rich, containing iron oxides (e.g., magnetite, wüstite) and iron sulfides (e.g., pyrrhotite, pentlandite). The fragmentary debris may be either fine-grained aggregates of olivine, magnetite, pyroxene, and occasionally pyrrhotite (derived from the meteorite matrix) or individual olivine and pyroxene grains (derived from meteorite inclusions).

¹San Jose State University, San Jose, California 95192

ORIGINAL PAGE IS
OF POOR QUALITY



Identification of the above kinds of ablation debris in the stratospheric particle collection was positively confirmed for many particles. The obvious ablation debris are spherules in the chondritic, FSN, and Fe-Ni groups of the stratospheric collection. The chondritic spherules are identified by their melt texture, the presence of olivine and magnetite, and spheroidal iron sulfides. The FSN and Fe-Ni spherules can be considered products of ablation solely by the presence of different stages of oxidized iron (e.g., magnetite, wüstite). Additional confirmation is supplied by the identical mineralogy found in artificial debris and the depletion of volatile sulfur in the FSN spherules. For the remaining stratospheric particles, chondritic aggregates (comprises about 1/2 the stratospheric collection), mafic silicates, and angular FSN's, there is some doubt if they are a special form of ablation debris or unaltered interplanetary dust. The issue is whether or not fragmentation produces quantities of unmelted grains that survive in the Earth's atmosphere. Unfortunately, we are now only able to unequivocally demonstrate that those particles with high ^4He content and those with unoxidized Fe-Ni mounds have never fragmented or ablated.

INTRODUCTION

Recent collections of 5- to 50- μ m particles from the stratosphere may soon be the object of intense research as a source of interplanetary dust, from which information may be gained on the origin of the solar system. These particles include both interplanetary dust and meteor ablation debris, and are now being collected at an altitude of 20 km with NASA's U-2 aircraft. To date, over 250 particles [Brownlee et al., 1976] have been collected that appear to be extraterrestrial. However, before the interplanetary dust can be studied in depth, it is necessary to identify and separate the meteor ablation debris from the collection.

To develop criteria for identifying meteor ablation debris, a systematic study of ablation products was initiated [Blanchard, 1969, 1972, 1973]. Fusion crusts of natural meteorites were compared with fusion crusts and ablation debris created in the laboratory. Comparisons between the fusion crusts of two carbonaceous chondrites, Allende and Murchison [Blanchard et al., 1974], and the laboratory-ablated olivine and pyroxene samples showed [Blanchard and Cunningham, 1974] that the ablated debris consisted predominantly of a recrystallized Fe-deficient olivine, magnetite, and glass. Similar comparisons between the fusion crusts of three Ni-Fe meteorites (Boguslavka, Norfolk, and N'Kandhla) with spherules from deep sea manganese nodules, and laboratory-ablated Fe and Ni-Fe metallurgical samples showed that the ablation debris of a Ni-Fe meteor consisted predominantly of magnetite, hematite, taenite (γ Ni-Fe, metal), and the disequilibrium-phase wüstite [FeO_{1-x} , Blanchard and Davis, 1978]. The majority of the stratospheric particles have elemental abundances and textures similar to the most primitive carbonaceous chondrites, which prompted another laboratory ablation study with an actual sample of the Murchison meteorite, a C2 carbonaceous chondrite

[Kyte, 1977]. It was concluded from these analyses that the following guidelines should be the basis for recognizing ablation debris from iron and silicate-rich meteoroids.

1. Occurrence of disequilibrium mineral phases (e.g., wüstite, glass, and zoned olivine) due to melting and rapid cooling.
2. Distinctive textures (e.g., zoned olivine surrounded by magnetite crystals in a groundmass of glass) produced by intergrown dissimilar phases.
3. Depletion and migration of volatile elements (e.g., S, C, H₂O) due to heating.
4. Fractionation and concentration of less-volatile elements in some mineral phases according to their affinity for oxygen (e.g., Ni-rich metal cores surrounded by Ni-poor iron oxides).

In this paper the differences between the stratospheric particles and the ablation debris that originates from meteoroids (especially carbonaceous chondrites) are compared in hopes of showing what fraction of the stratospheric particles represents unaltered interplanetary dust and what fraction represents debris ablated from meteoroids.

PROCEDURE

The Murchison meteorite was selected for artificial ablation experiments because there were many similarities between the stratospheric particles and carbonaceous chondrites, and the chemistry and mineralogy of this chondrite has been well studied. The Murchison meteorite contains a mixture of high- and low-temperature condensates and is composed mainly of a fine-grained, hydrated, layer-lattice silicate (Fe-rich, Al-poor chamosite) with inclusions of olivine and Ca-poor pyroxene [Fuchs et al., 1973]. There is little troilite,

magnetite, and free metal in the meteorite. Most of the S and some of the Fe occur in a poorly characterized, amorphous Fe-S-O phase in the chamosite matrix. The olivine-to-pyroxene ratio is 2:1. These two minerals are typically Fe-poor with a range of 1-5% mole fraction of Fa (olivine) or Fs (pyroxene), although more Fe-rich grains do occur.

For ablation studies, a 406-g specimen (#Me 2684) of the Murchison meteorite was broken by hand and trimmed to 62 g with a diamond-impregnated copper wire. The sample was ablated (Figure 1) using a plasma beam consisting of ionized air, argon, and electrons in the 1.3-cm-diameter constricted-arc jet facility at NASA Ames Research Center [Shepard et al., 1967]. The desired conditions were to simulate a 30-cm-diameter meteor traveling 12 km/s at an altitude of 70 km. Unfortunately, with this facility, we were unable to achieve a sufficiently high stagnation pressure in the gas cap, and the pressures on the sample were lower, simulating an altitude somewhat above 100 km (Carlson, personal communication). Thus, this experiment primarily simulated heating rates and not pressures.

Ablation debris was collected from the chamber for analysis. Water-cooled copper trays were placed directly behind and below the ablating model; chrome-plated trays were placed along the sides and rear of the chamber. These trays collected debris falling directly off of the ablating model. Debris was also recovered from the floor and walls of the chamber. The experiment lasted only several seconds, after which time the sample was nearly consumed (but still had an artificial fusion crust for analysis), and the copper holder began to ablate.

Since March 1974, the stratospheric particles have been collected by NASA U-2 aircraft with an inertial impaction device [Ferry and Lem, 1974]

designed for collecting submicron aerosols. This device was modified to expose larger surface areas and to collect larger (up to 50 μm) particles [Brownlee et al., 1976]. The initial characterization of these particles was performed by Brownlee et al. [1976], who used a scanning electron microscope (SEM) to select the particles and screen out likely contaminants. X-ray energy dispersive elemental analysis was used to categorize the textures and analyze the elemental composition of these particles. For this paper representative particles of the U-2 collection were analyzed by X-ray diffraction to characterize the particle's mineralogy. The stratospheric particles were then compared with natural and artificial fusion crusts and ablation debris examined from Murchison and previous studies.

Analyses were performed with natural and artificial fusion crusts, hundreds of spherules and fragmentary particles of artificial ablation debris, and selected stratospheric particles. Textural and morphological features were examined by optical microscopy and the scanning electron microscopy (SEM). Qualitative elemental analyses were performed with energy dispersive X-ray detectors in the SEM (Joelco, JSMU 3) and the electron microprobe (MAC 400). This permitted estimates of relative elemental weight fractions for the ablation debris and the intergrown phases in the fusion crusts. Original meteorite samples (not containing any fusion crust) and artificial ablation debris were studied by bulk analyses, using X-ray fluorescence. Bulk analyses were performed under contract by Gary G. Cunningham, Geology Department, University of Oregon. Minerals in the artificial ablation debris and stratospheric particles were identified by X-ray diffraction techniques described by Blanchard [1972]. Using the 57.3-mm Debye-Scherrer camera, the stratospheric particles were exposed to X-rays for 4 days to 21 days and the

artificial ablation debris for 4 hr to 5 days. Every precaution was taken to exclude contaminants from the analyses of the artificial ablation debris. Particles from the arc-jet chamber were considered as contaminants unless their elemental abundances closely matched the original meteorite, or they otherwise were demonstrated to have been created during the ablation experiment (e.g., spherule shaped).

CHARACTERISTICS OF ABLATION DEBRIS FROM CARBONACEOUS CHONDRITES

The natural and artificial fusion crusts are very similar and the ablation debris collected in the Murchison experiment closely resembles the fusion crust of the Murchison meteorite. Although magnetite is not as common in the outer zone of the artificial fusion crust as in the natural fusion crust, it is ubiquitous in the recrystallized ablation debris.

Murchison Fusion Crusts.

The natural and artificial fusion crusts are similar and can be divided into two zones based upon the amount of heat they experience. The outer zone (Figure 2, #1), the higher-temperature zone, was originally molten but solidified after ablation to form a fusion crust with discontinuous glassy and lobate protuberances often connected by thin glassy membranes. The inner zone (Figure 2, #2), the lower-temperature zone, shows signs of partial melting, but not to any great extent because there are some unaltered olivine grains.

The outer zone of the natural and artificial fusion crusts have common mineral phases: magnetite, olivine, and glass. The magnetite crystals are dominant in natural fusion crusts (Figure 3) and form chains of equant, cubic, micron-sized crystals; in artificial fusion crusts, magnetite crystals are a minor phase and occur as submicron intergrowths. Olivine occurs as subhedral

and euhedral crystals up to 10 μm . These crystals have a zoned composition, with Fo_{70} at their centers and progressively more Fe-rich at their outer rims (Figure 4). Glass occurs as an interstitial matrix material surrounding the magnetite and olivine crystals with a composition of Fe, Si (major); Ca, Al (minor); and Mg (trace).

The inner zone is commonly transected by fractures and elongated holes (Figure 5) perpendicular to the surface of the fusion crust through which vaporizing volatiles have escaped. In natural and artificial fusion crusts, troilite, recrystallized (Figure 2) in lenses and pods, has invaded the fractures and holes of the inner zone.

Murchison Ablation Debris.

The ablation debris has been divided into two morphological groups: (1) spherules and spheroidal particles that have solidified from molten droplets, and (2) fragmentary debris, angular particles that never completely melted.

Spherules. Spherules, from 1 μm to 1 mm in diameter, are typically grayish black with a slight luster. The surface textures shown by SEM in Figure 6 were variable.

The two types of spherules in ablation debris (silicate and sulfide) are shown in Table 1. Silicates predominate over the sulfides by about 50:1. Silicate spherules are similar in composition to the original meteorite except S has been depleted. The major elements are Fe, Si, and Mg; minor elements are Ca and Al; common trace elements are Ni and Cr. These spherules contain olivine ($\sim\text{Fo}_{70}$), glass, and magnetite (Figure 6a). Many silicate spherules (20%) contain inclusions of the same sulfide phase (Figure 6c), which forms the sulfide spherules. Sulfide spherules (Figure 6b) are rich in Fe and have

variable amounts of S and Ni. These spherules contain magnetite, wüstite, pyrrhotite, and pentlandite; occasionally, all of these minerals occur in the same spherule. The pentlandite cell dimensions are large, indicating an Fe/Ni atomic ratio >2 .

Fragmentary Debris. About 75% of this material is typically a fine-grained black, nonporous aggregate containing several minerals (Table 1). Occasionally, these particles are large (≤ 5 mm in diameter), indicating that the meteorite sample was fragmenting well back of the fusion crust. However, the smaller fraction (<150 μm in diameter) predominates and shows little or no sign of melting. The elemental abundance and the fine-grained textures of these aggregates indicate they were originally part of the fine-grained matrix of the meteorite. In addition to this fine-grained fragmentary material, single grains of mafic silicates (olivine and enstatite), high in Si and Mg and usually low in Fe, are common (~25%). These mafic silicates (Table 1) are transparent with a reddish tinge (caused by heating) and have angular or rounded edges. The fine-grained debris typically contains Fe-poor olivine, magnetite, enstatite, and occasionally pyrrhotite. An SEM micrograph of a typical fine-grained fragmentary particle is shown in Figure 7. Occasionally, some of the fine-grained debris can be found with a fusion crust on one side (Figure 8).

Mineral Associations.

Four different mineral assemblages have been identified in the artificial ablation debris (Table 2): (1) olivine-magnetite-glass, in nearly all spherules; (2) olivine-magnetite-enstatite-pyrrhotite in 3/4 of the fragmentary debris; (3) olivine-pyroxene unmelted grains in about 1/4 of the fragmentary

debris; and (4) iron oxides-iron sulfides in few spherules but a common accessory in assemblage (1). These mineral assemblages represent the effects of heating and fragmentation experienced by the sample during ablation.

Bulk Analyses.

Bulk analyses of the original meteorite and the spherules were used to interpret general trends in the ablation process. The bulk analyses values for the original meteorite in this study agree with the values of Fuchs et al. [1973] and Jarosewich [Fuchs et al., 1973]. Although there is a trend for depletion of volatile elements like S, Na, and H₂O, there are only minor changes in relative proportions of Mg, Al, Ca, and Fe to Si in the spherules compared with the original meteorite.

Origin of Mineral Associations Produced by Ablation of Murchison Meteorite.

The olivine-magnetite-glass assemblage was formed from molten droplets derived from the outer zone of the fusion crust. The olivine is a recrystallized Fe-deficient forsterite, which forms from destroyed matrix materials (layer-lattice hydrated silicates, olivine, and pyroxene). The glass forms only when rapid quenching occurs. The glass is abundant in the fusion crust and the ablation debris. Magnetite is an abundant mineral in fusion crusts (Figure 3) and artificial ablation debris (Figure 9) because it forms in the melt after many other minerals have been destroyed or oxidized. Magnetite is formed (1) by a combination of incongruent melting and solid-state diffusion of the Fe-rich silicate minerals (olivine, pyroxene, hydrated silicates); (2) by simultaneous destruction and oxidation of the iron sulfides (pyrrhotite, troilite, and the Fe-S-O phase); or (3) when metallic Ni-Fe and magnetite are melted

and recrystallized in an atmosphere having suitable oxygen partial pressures. This assemblage has been previously reported during studies of the natural fusion crusts of the chondritic meteorites, Allende and Murchison [Blanchard and Cunningham, 1974]. Further, an olivine-magnetite-glass assemblage has been observed in the fusion crust of other chondrites [Orgueil, Brownlee et al., 1975; Warrenton, Ramdohr, 1967], and magnetite is common in the debris from the Tunguska meteorite fall [Florenskiy et al., 1968; Florenskiy and Ivanov, 1970]. A somewhat similar assemblage of minerals (olivine-enstatite-magnetite-wustite-glass) was described by Yudin [1955] in the fusion crust of Kunashak, an ordinary chondrite. These observations demonstrate that the magnetite-olivine-glass assemblage is a typical product of the ablation process from chondritic meteorites.

The olivine-magnetite-enstatite-pyrrhotite assemblage was formed from fine-grained matrix materials that were heated in the inner zone of the fusion crust. The olivine and magnetite formed from the original chamosite matrix by incongruent melting and solid state diffusion, as described earlier. Fuchs et al. [1973] heated Murchison matrix material to 450°C forming olivine and magnetite from the chamosite and, whenever the poorly characterized Fe-S-O phase was present, FeS was formed. This low temperature heating is effective at forming the sulfide-rich veins observed in the fusion-crust inner zone and the pyrrhotite in the fragmentary debris. The enstatite and some of the olivine identified probably represent unaltered minute grains of these minerals within the fine-grained fragmentary debris.

The olivine-pyroxene assemblage is composed of unmelted grains of mafic silicates (olivine, enstatite) in which individual particles have separated from the sample by fragmentation without having been altered by heating. The

existence of both types of fragmentary debris demonstrates that fragmentation of the sample allows the fragments to escape the melting process.

Occasionally, some mafic grains may show rounded edges, suggesting they were only briefly exposed to high temperatures. In the artificial ablation experiment, fragments needed only to escape the arc jet plasma to avoid melting and vaporization. The low impact pressures in this experiment had a significant effect on the composition of the melted debris and the amount of unmelted debris produced. First, the partial pressure of oxygen was lower than in the real environment for this altitude, so oxidation of the sample was not extensive. Second, lower gas-cap pressures with these heating rates favored melting and vaporization rather than fragmentation in the ablation process. Because the sample was fragile, higher impact pressures would have destroyed it faster, producing even larger quantities of fragmented debris. In this experiment, we demonstrated that unmelted particles can survive meteor ablation in the laboratory. If this is possible in nature, then it is likely to occur when the gas-cap pressures are high.

The iron oxide-iron sulfide assemblage is also a product of the ablation process. The sulfides and oxides always occur together in these particles. The sulfides were formed in the inner zone of the fusion crust as the matrix was heated. During this time, the troilite and poorly characterized Fe-S-O phase melted, forming the sulfide veins that migrated inwards. These particles did not form in the outer zone because the sulfides would not survive the high temperatures. A process allowing these sulfides to form requires low-temperature heating and rapid cooling. When the ablating sample fragmented, exposing the inner zone of the fusion crust, droplets were produced, which sprayed out from sulfide veins forming the S-rich spherules.

Silicate spherules with the sulfide inclusions formed when silicate droplets containing sulfide inclusions fragmented from the inner zone, melted, and cooled rapidly. Liquid droplets of silicate and sulfide phases may also have combined during flight after leaving the sample. The iron oxides are not associated with silicate minerals or glass, but formed from a metal-sulfide melt from which some sulfur was vaporized and Fe was oxidized.

CHARACTERISTICS OF THE STRATOSPHERIC DUST PARTICLES

Brownlee et al. [1976] used elemental abundances and textural features to describe 250 particles collected by the U-2 aircraft from the stratosphere thought to contain interplanetary dust. With these two parameters, the particles have been classified into five groups: chondritic (60%), FSN (30%), mafic silicates (6%), Fe-Ni (3%), and others (1%).

Chondritic Particles

Chondritic particles are either aggregates (90%) or ablation debris (10%). Chondritic aggregates (Figure 10) are aggregates of particles 1000 \AA and are typically compact with little pore space; some, however, are porous (Figure 11). Their elemental abundances are within a factor of two of chondritic meteorites for Fe, Mg, Si, C, S, Ca, and Ni. Carbon ranges from 2-15% in those particles this element was measured. Half of the ten particles analyzed for ^4He contained this element in concentrations comparable with lunar soils. The mineralogy of these chondritic aggregates include hydrated silicates, olivine, magnetite, and pyrrhotite. The chondritic ablation particles are spherules (Figure 12) or spheroidal, verifying they were once molten. None of the particles are porous or contain S, although an inclusion that contained Ni-Fe and a small amount of S was

found in one spherule [Brownlee personal communication]. The minerals in these particles include olivine and magnetite.

FSN Particles.

FSN particles exist in many forms. Most are spherules (Figure 13), although there are platelets (Figure 14) and crystals (Figure 15). The particles are rich in Fe, Ni, and S. Sulfur is often deficient relative to stoichiometric FeS. Sulfur content varies greatly and is sometimes so low that FSN particles are similar to Ni-Fe particles. Nonspherical particles are sometimes intimately associated with the chondritic aggregates. The minerals in these particles include pyrrhotite, pentlandite, magnetite, and wüstite.

Mafic Silicates.

Mafic silicates exist in many forms, often with clumps of chondritic aggregates on their surface (Figure 16). Half of the particles appear to contain pyroxene while the other half appear to contain olivine. The minerals in these particles include olivine, pyroxene, magnetite, and pyrrhotite.

Fe-Ni Particles.

Fe-Ni particles are mostly spheres containing taenite, magnetite, and wüstite.

Other Particles.

This group classification contains a few chondritic silicate particles that have numerous Fe-Ni mounds (Figure 17) on their surface. Taenite and

pyrrhotite have been identified in one of these particles; the absence of any iron oxides is a significant characteristic and indicative of the origin of these particles.

SIMILARITIES BETWEEN THE STRATOSPHERIC DUST PARTICLES AND NATURAL
AND ARTIFICIAL ABLATION DEBRIS FROM CARBONACEOUS CHONDRITES
AND IRON METEORITES

The textural, elemental, and mineralogical characteristics of some of the particles collected from the stratosphere by the U-2 aircraft are similar to the artificial ablation debris and natural fusion crusts of the chondritic and iron meteorites we examined. Four groups of particles (chondritic, Fe-Ni, FSN, and mafic silicates) of the five recognized in the stratospheric collection compare especially well (Table 3) with the mineral assemblages (olivine-magnetite-enstatite-pyrrhotite, olivine-magnetite-glass, iron oxides-iron sulfides, magnetite-hematite-wüstite-taenite, and olivine-pyroxene) produced by artificial ablation from the Murchison meteorite and the Ni-Fe samples.

Chondritic particles from the stratosphere resemble the olivine-magnetite-enstatite-pyrrhotite and the olivine-magnetite-glass mineral assemblages from laboratory-generated ablation and fragmentation debris of the Murchison meteorite. The fine-grained, nonporous, stratospheric chondritic aggregates have textures (Figure 10) similar to the fine-grained, nonporous particles (olivine-magnetite-enstatite-pyrrhotite) produced by laboratory-generated fragmentation of the Murchison matrix (Figures 7 and 8). Those stratospheric chondritic spherules, tentatively identified as natural ablation debris (Figure 12) match the spherules and fusion crust from

Murchison ablated in the laboratory (Figure 6). The elemental content (major Fe, Si, Mg; minor Ca, Al, and occasionally S) for these particles and the mineralogy (olivine, pyroxene, serpentine or chamosite, magnetite, and pyrrhotite) for these particles are nearly identical (Table 3).

The Fe-Ni particles collected from the stratosphere resemble the magnetite-hematite-wüstite-taenite mineral assemblage occurring in fusion crusts of natural and artificial Ni-Fe meteorites, the artificial ablation debris produced in the laboratory [Blanchard and Davis, 1978], and the spheres in deep-sea sediments [Millard and Finkelman, 1970; Finkelman, 1972]. The minerals in the Fe-Ni stratospheric spheres are taenite, magnetite, and wüstite. The iron oxides in these particles, especially wüstite, indicate an ablation origin from an iron meteorite. Wüstite is a metastable iron oxide that is preserved only by rapid cooling of liquid iron oxide in an atmosphere in which the oxygen pressure is insufficient to allow formation of the more stable magnetite or hematite [Blanchard, 1970, 1972]. The absence of hematite in these spherules is not significant because hematite is rare as a primary mineral in ablation products.

The FSN, and indirectly, Fe-Ni particles collected from the stratosphere resemble the iron oxides-iron sulfides mineral assemblage in the laboratory-produced Murchison fusion crust and artificial ablation debris. As S is depleted and Fe is oxidized, the FSN particles grade into the Fe-Ni particles. The mineralogy of the stratospheric FSN particles and the laboratory-produced Murchison iron oxides-iron sulfides have the same common minerals (i.e., pentlandite, pyrrhotite, magnetite, and wüstite) and they have similar elemental abundances. Predominantly, the FSN particles are spheroidal (Figure 13, stratospheric FSN; Figure 6b, Murchison ablation), but the

stratospheric particles include octahedron crystals (Figure 15) and platelets (Figure 14) for which there is no counterpart in the laboratory-produced Murchison ablation and fragmentation debris. Also, the inclusions of iron oxides-iron sulfides in the Murchison fusion crust (Figure 2) and ablation spherules (Figures 6c, 9) from the laboratory are similar to iron sulfide inclusions in chondritic spherules from the stratosphere.

The mafic silicate stratospheric particles (Figure 16) resemble the unmelted olivine-pyroxene fragmentary debris from Murchison generated in the laboratory. Both types have similar elements, textures, and minerals. However, the submicron particles adhering to the surface of the mafic silicates have never been seen in the artificial ablation debris.

The stratospheric particles classified as "others" appear to be unique. No equivalent to the Ni-Fe mounds found in the stratospheric particles (Figure 17) exists in the laboratory-generated ablation debris from Murchison. The Ni-Fe would have been oxidized to form iron oxides if it had been ablated in an environment containing oxygen.

CONCLUSIONS

Identification of ablation debris in the stratospheric particle collection was positively confirmed for many particles from each group. The obvious ablation debris are chondritic ablation, FSN spherules, and Fe-Ni spherules. The chondritic ablation particles are identified by their melt texture, the presence of olivine and magnetite, and by the spheroidal iron sulfide inclusions. The FSN and Fe-Ni spherules can be considered products of ablation solely by the presence of different stages of oxidized iron (i.e., magnetite, wüstite). Additional confirmation is the depletion of volatile S in the FSN spherules.

For the remaining particles — chondritic aggregates (comprises about one half the stratospheric collection), mafic silicates, and angular FSN — there is some doubt if they are a special form of ablation debris or unaltered interplanetary dust. The issue is whether or not fragmentation produces quantities of unmelted grains. The data of Cepilecha and McCroskey [1967] has shown that many fireballs undergo gross fragmentation in the upper atmosphere, and supports the production of fragmentary debris. Even at the low impact pressures of the laboratory ablation experiment, there was as much unmelted debris produced by fragmentation of the Murchison sample as there was produced by melting. However, the main question is whether any of this fragmentary debris can survive. The particles most likely to survive unaltered after fragmentation should be the mafic silicates because they have high melting temperatures. One interesting possibility is that mafic silicates could survive as relict grains within larger spherules. However, this has not yet been observed in either the stratospheric particles or the Murchison debris. This phenomenon could occur if gross fragmentation produced a particle composed of fine-grained matrix with a mafic silicate grain inclusion. The matrix could then melt at lower temperatures, forming a spherule and produce an inclusion of olivine or pyroxene.

Although we now have adequate mineralogical criteria for recognizing ablation debris from iron and chondritic meteorites, only part of the stratospheric particles meet these criteria well. Unfortunately, we are now only able to unequivocally demonstrate that those particles with a high ^4He content and those with unoxidized Fe-Ni inclusions have never experienced fragmentation or ablation processes. Clearly, ^4He is so volatile that it could only occur in unaltered interplanetary dust. Collection and analyses

of debris from the atmosphere in the wake of a large fireball event would help to characterize typical products from the fragmentation and ablation processes.

Acknowledgments. Donald E. Brownlee of the Astronomy Department, University of Washington, provided the extraterrestrial stratospheric particles analyzed in this study, and valuable insight concerning these particles and their relationship to ablation debris. Dr. Edward Olsen, Curator of Mineralogy, Field Museum of Natural History, kindly supplied the sample of the Murchison meteorite that was ablated and analyzed in this study. Special thanks are due to William C. A. Carlson, Assistant Chief, Thermo-Physics Facilities Branch, and Howard K. Larson, Chief, Entry Technology Branch, Ames Research Center, without whose aid the ablation experiment would not have been possible. The analytical studies were performed in the Planetology Branch laboratories at Ames Research Center where support services were supplied by Homer Y. Lem (scanning electron microscopy), of LFE-Environmental Analysis Laboratories, Richmond, California, under contract NAS 2-9325. This research investigation was supported in part by NASA-Ames University Consortium Agreement (NCA 2-OR675-612).

References

- Blanchard, M. B., Preliminary results of artificial ablation, Meteoritics, 4, 261, 1969.
- Blanchard, M. B., Wüstite - a common occurrence in artificial meteor ablation products, Meteoritics, 5, 181, 1970.
- Blanchard, M. B., Artificial meteor ablation studies: iron oxides, J. Geophys. Res., 77, 2442, 1972.
- Blanchard, M. B., Artificial meteor ablation studies, in Hemenway, C. L., Millman, P. M., and Cook, A. F., eds., Evolutionary and physical properties of meteoroids, NASA SP-319, 241, 1973.
- Blanchard, M. B., and Cunningham, G. G., Artificial meteor ablation studies: olivine, J. Geophys. Res., 79, 3973, 1974.
- Blanchard, M. B., Cunningham, G. G., and Brownlee, D. E., Comparison of a fusion crust produced by artificial ablation of an olivine with fusion crusts on the Allende and Murchison meteorites, Meteoritics, 9, 316, 1974.
- Blanchard, M. B., and Davis, A. S., Analysis of ablation debris from natural and artificial iron meteorites, J. Geophys. Res., 83, 1793, 1978.
- Brownlee, D. E., Blanchard, M. B., Cunningham, G. G., Beauchamp, R. H., and Fruland, R., Criteria for identification of ablation debris from primitive meteoritic bodies, J. Geophys. Res., 80, 4917, 1975.
- Brownlee, D. E., Tomandl, D., Blanchard, M. B., Ferry, G. V., and Kyte, F. T., An atlas of extraterrestrial particles collected with NASA U-2 aircraft - 1974-1976, NASA TM X-73,152, 1976.

- Cepplecha, Z., and McCroskey, R. E., Fireball end heights: a diagnostic for the structure of meteoric material, Smithsonian Astrophysical Observatory, Center of Astrophysics, preprint, 442, 1976.
- Ferry, G. V., and Lem. H. Y., Aerosols at 20 km altitude, Proc. 2nd Intl. Conf. on Env. Impact of Aerospace Ops. in High Atmos., San Diego, Calif., July, 1974, Amer. Meteor. Soc., 23, 1974
- Finkelman, R. B., Relationship between manganese nodules and cosmic spherules, Marine Tech. J., 6, 34, 1972.
- Florenskiy, K. P., Ivanov, A. V., Koriva, O. A., and Zaslavskaya, N., I., Phase composition of the extraterrestrial dust in the region of the Tunguska fall, Geochem. Inc., 5, 997, 1968.
- Florenskiy, K. P., and Ivanov, A. V., Differentiation of meteoritic matter in the earth's atmosphere, Meteoritika, 30, 104, 1972, (NASA Tech. Transl. TTF-14, 138, 1, 1972).
- Fuchs, L. H., Olsen, E., and Jensen, K. J., Mineralogy, mineral chemistry, and composition of the Murchison (C2) meteorite, Smithsonian Institution, Smithsonian Contributions to the Earth Sciences, No. 10, 1973.
- Kyte, F. T., On the origin of extraterrestrial stratospheric particles: interplanetary dust or meteor ablation debris?, M.S. thesis, Geology Dept., San Jose State University, San Jose, Calif., 1977.
- Millard, H. T., and Finkelman, R. B., Chemical and mineralogical compositions of cosmic and terrestrial spherules from a marine sediment, J. Geophys. Res., 75, 2125, 1970.
- Ramdohr, P., Die schmelzkruste der meteoriten, Earth Planet. Sci. Lett., 2, 197, 1967.

Shepard, C. E., Vorreiter, J. W., Stine, H. A., and Winovich, W. I., A study of artificial meteors as ablators, NASA Tech. Note D-3754, 1977.

Yudin, I. A., Kora playlenya kamennogo meteorita Kunashak, Meteoritika, 13, 143, 1955.

TABLE 1. Qualitative Elemental Abundance and Mineralogy of the Artificial
Ablation Debris

Types of Ablation Debris	Elemental* Abundances								Mineralogy	
	Mg	Al	Si	S	Ca	Cr	Fe	Ni		
<u>Spherules</u>	High	Low	High	Low	Low	Low	High	Low		Olivine with accessory magnetite and glass
Silicates	High	Low	High	Low	Low	Low	High	Low		
Sulfides	Low	Low	Low	High	Low	Low	High	Low		Magnetite or wustite, or both, and pentlandite or pyrrhotite, or both
Fragmentary Debris	Low	Low	Low	High	Low	Low	High	Low		
Fine-grained Aggregates	High	Low	High	Low	Low	Low	High	Low		Olivine and magnetite with some enstatite and pyrrhotite (rare)
Mafic Silicates	High	Low	High	Low	Low	Low	High	Low		

*The white sections of the histogram bars represent the maximum variation of that element in the group of particles; the black sections represent the average elemental concentration of that element in the group of particles.

TABLE 2. Occurrence of the Mineral Assemblages in the Artificial Ablation
Debris from the Murchison Meteorite

Predominant Mineral Associations	Occurrence
Olivine-magnetite-glass	Fusion crust, and spherules (nearly 100%).
Olivine-magnetite-enstatite-pyrrhotite	Fine-grained aggregates (75% of fragmentary debris).
Olivine-pyroxene	Fine-grained mafic debris (25% of fragmentary debris).
Iron oxides-iron sulfides	Spherules (minor), and common inclusions in fusion crust and silicate spherules.

TABLE 3. Comparison Between the Stratospheric Dust Particles and the Artificial Ablation Debris Produced from Murchison and Ni-Fe Metallurgical Samples [Blanchard and Davis, 1978].

Stratospheric Dust Particles			Artificial Ablation and Fragmentation Debris from Carbonaceous Chondrites and Iron Meteorites				
Group	Typical Occurrence	Typical Elements	Typical Mineralogy	Mineral Association	Typical Occurrence	Typical Elements	Typical Mineralogy
<u>Chondritic</u>							
Aggregates	Fine-grained porous and nonporous	Major: Si, Mg, Fe, S Minor: Ca, Al, Cr, Ni (occasionally He)	Olivine, serpentine pyrrhotite, magnetite	Olivine-magnetite-enstatite-pyrrhotite	Fine-grained aggregates, nonporous	Major: Fe, Si, S, Mg Minor: Ca, Al, S	Olivine, magnetite, pyroxene, chamosite, pyrrhotite
Ablation	Spheroidal, melted crust	Major: Fe, Si, Mg Minor: Ca, Al, Ni, Cr	Olivine, magnetite	Olivine-magnetite-glass	Fusion crust, spherules	Major: Fe, Si, Mg Minor: Ca, Al	Olivine, magnetite
FSN	Spheroidal, crystals, and platelets	Major: Fe, S, Ni Minor: S (occasionally)	Pyrrhotite, pentlandite, magnetite, wüstite	Iron oxides-iron sulfides	Spherules, inclusions in spherules and fusion crust	Major: Fe, S, Ni	Magnetite, wüstite, pyrrhotite, pentlandite
Fe-Ni	Spheroidal	Major: Fe, Ni	Taenite, magnetite wüstite	Magnetite-hematite-wüstite-taenite	Spherules	Major: Fe, Ni	Magnetite, hematite, wüstite, taenite
Mafic Silicates	Subangular, crystals with adhering chondritic material	Major: Si, Mg, Fe Minor: Ca, Al, S	Olivine, pyroxene, clinenstatite, magnetite, pyrrhotite	Olivine-pyroxene	Single crystals (fragmentary)	Major: Si, Mg, Fe Minor: Ca	Olivine, pyroxene
Others	Spheroidal or aggregates with adhering Ni-Fe mounds	Major: Si, Mg, Fe Minor: S, Ni	Olivine or glass, pyrrhotite, taenite				

ORIGINAL PAGE IS OF POOR QUALITY

FIGURE CAPTIONS

Fig. 1. Schematic diagram of constricted-arc supersonic jet with sample of Murchison meteorite ablating.

Fig. 2. Reflected light photomicrograph showing the outer (#1) and inner (#2) zones of the fusion crust of the Murchison meteorite. Bright grains in the inner zone are inclusions of iron sulfides invading the fractures and voids.

Fig. 3. SEM image of the natural fusion crust on the Murchison meteorite. The small equant, brightly colored grains are magnetite. The larger crystal outlines shown in light grey are recrystallized olivine grains. The darker grey interstitial material is glass.

Fig. 4. SEM image of the artificial fusion crust of the Murchison meteorite. The large crystal outlines shown in light grey are zoned olivine grains. These grains are enriched in Fe at the outer boundaries.

Fig. 5. SEM image of the natural fusion crust of the Murchison meteorite. The inner zone is characterized by voids and fractures through which vaporizing volatiles escape.

Fig. 6. SEM images of spherules ablated from the Murchison meteorite: (a) silicate sphere composed of olivine, glass and magnetite (bright grains at surface); (b) sulfide sphere composed of magnetite, pyrrhotite, and wüstite; (c) silicate spherule with an inclusion of the sulfide phase exposed at its surface.

Fig. 7. SEM image of the most common type of fragmentary debris, a nonporous, fine-grained particle containing micron grains of olivine, magnetite, enstatite, and occasionally pyrrhotite.

Fig. 8. SEM image of a fragmentary particle from the Murchison meteorite. Only one side of this particle shows evidence of melting, shown by a smooth fusion crust with numerous voids where volatiles have escaped.

Fig. 9. SEM image of a polished section of a silicate spherule produced by artificial ablation of the Murchison meteorite. The large grey crystals are zoned olivine, the small bright crystals are magnetite, and the dark matrix is glass. The spherical inclusion is composed of iron sulfides but its outer rim has been altered to magnetite.

Fig. 10. SEM image of a chondritic aggregate, nonporous particle from the U-2 stratospheric particle collection. Major elements are Si, Fe, Mg, S; minor elements are Ca, Al, Ni [Brownlee et al., 1976].

Fig. 11. SEM image of a chondritic aggregate, of unusually high porosity, from the U-2 stratospheric particle collection. Major elements are Si, Fe, S, Mg; minor elements are Ca, Ni, Al [Brownlee et al., 1976].

Fig. 12. SEM image of a chondritic ablation particle, spheroidal and showing submicron magnetite grains, from the U-2 stratospheric particle collection. Major elements are Fe, Si; minor elements are Mg, Ca, Al, Cr [Brownlee et al., 1976].

Fig. 13. SEM image of a FSN spherule from the U-2 stratospheric particle collection. Major elements are Fe, S; minor element is Ni [Brownlee et al., 1976].

Fig. 14. SEM image of an unusual FSN particle with platelet-like structure from the U-2 stratospheric particle collection [Brownlee et al., 1976].

Fig. 15. SEM image of an unusual FSN particle, with octahedron and cubic crystal faces, from the U-2 stratospheric particle collection. Major elements are Fe, S; minor element is Ni [Brownlee et al., 1976].

Fig. 16. SEM image of a mafic silicate grain with adhering chondritic aggregate particles from the U-2 stratospheric particle collection. Mafic silicate major elements are Mg, Si; a minor element is Fe. Chondritic particle major elements are Si, Fe, Mg, S; minor elements are Ca, Al, Ni [Brownlee et al., 1976].

Fig. 17. SEM image of an unusual round chondritic particle covered with Fe-Ni mounds. Major elements are Si, Mg, Fe; minor elements are Ca, Al, Ni, and Cr [Brownlee et al., 1976].

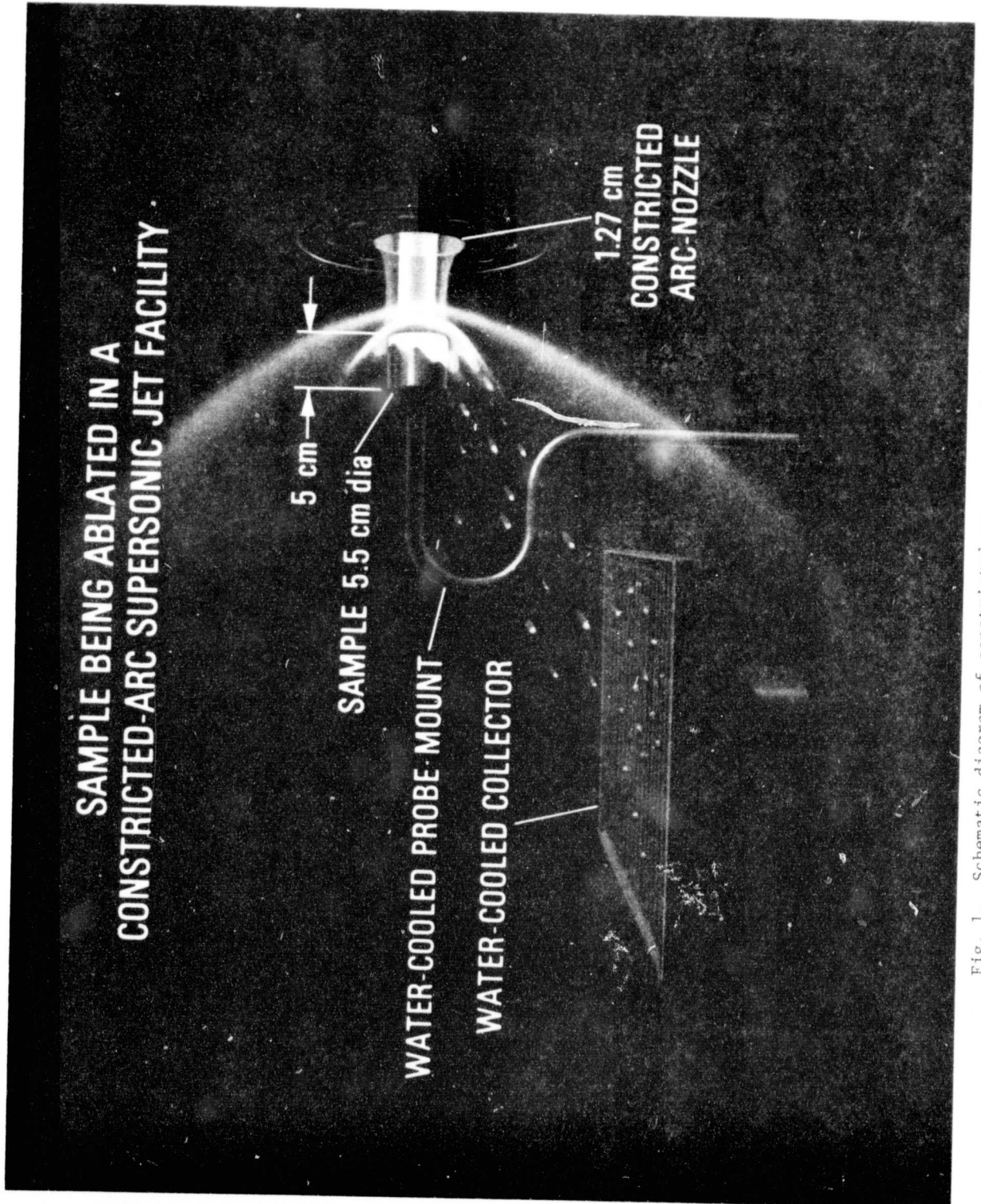


Fig. 1. Schematic diagram of constricted-arc supersonic jet with sample of Murchison meteorite ablating.



Fig. 2. Reflected light photomicrograph showing the outer (#1) and inner (#2) zones of the fusion crust of the Murchison meteorite. Bright grains in the inner zone are inclusions of iron sulfides invading the fractures and voids.

ORIGINAL PAGE IS
OF POOR QUALITY

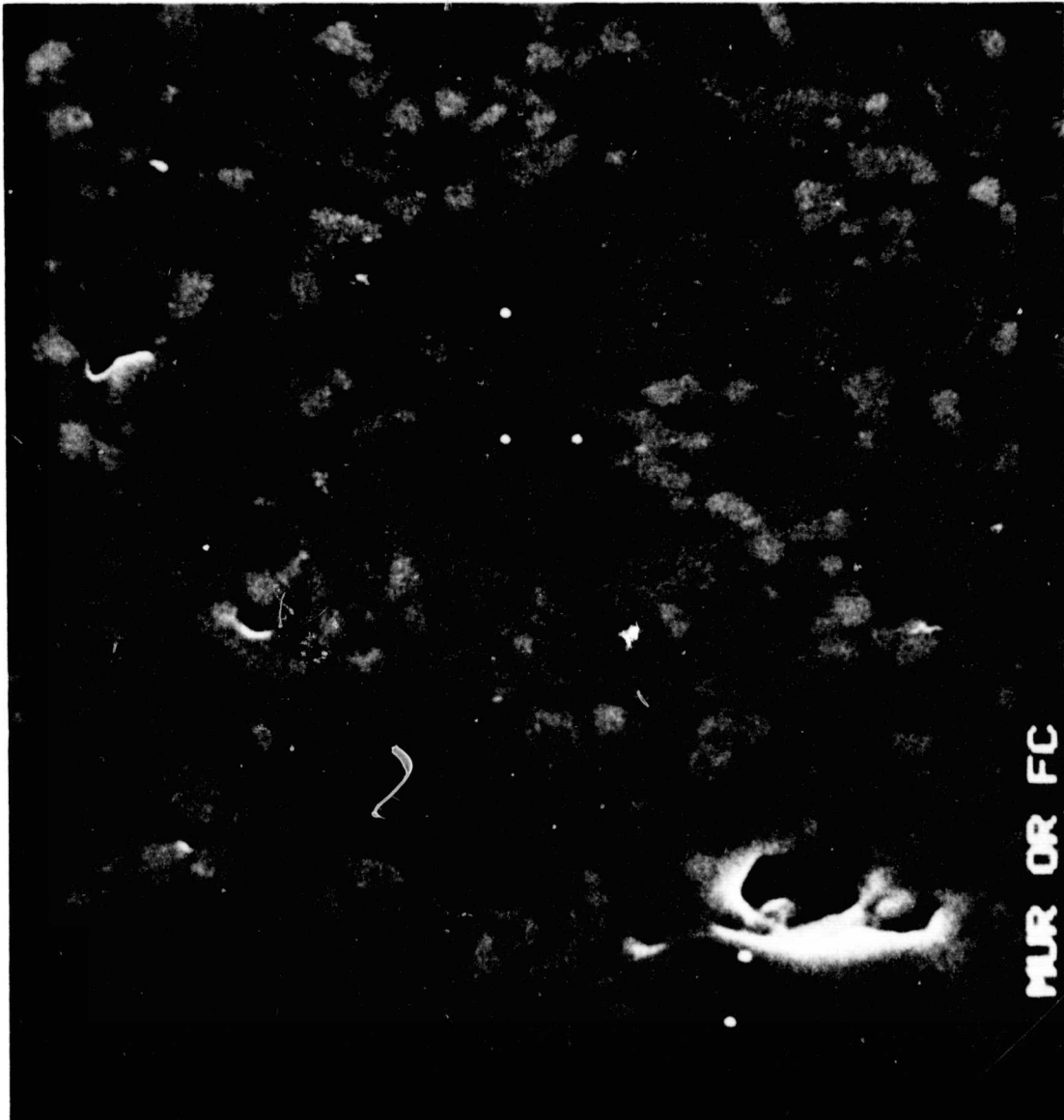


Fig. 3. SEM image of the natural fusion crust on the Murchison meteorite. The small equant, brightly colored grains are magnetite. The larger crystal outlines shown in light gray are recrystallized olivine grains. The darker grey interstitial material is glass.

ORIGINAL PAGE IS
OF POOR QUALITY

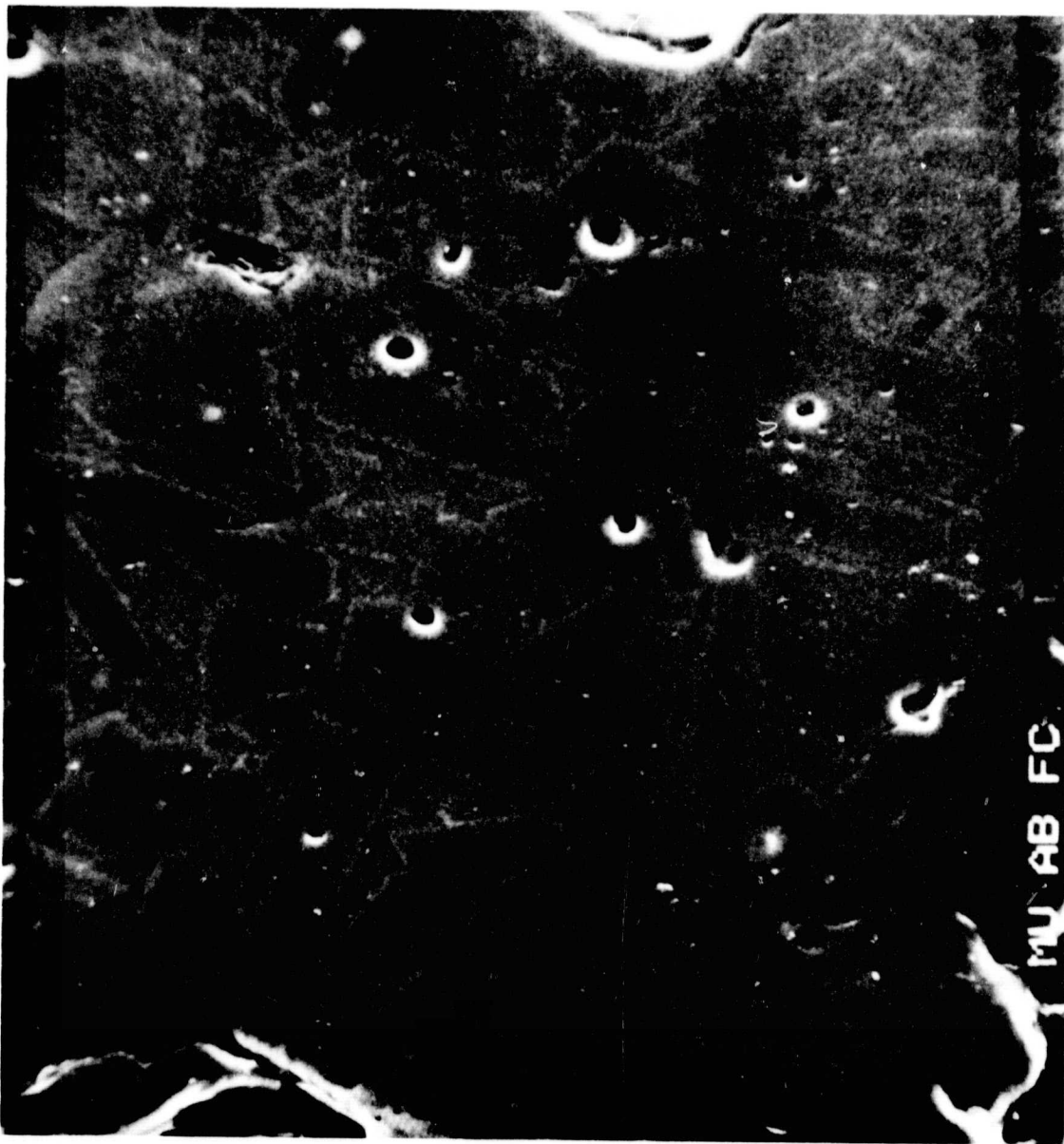


Fig. 4. SEM image of the artificial fusion crust of the Murchison meteorite. The large crystal outlines shown in light grey are zoned olivine grains. These grains are enriched in Fe at the outer boundaries.

ORIGINAL PAGE IS
OF POOR QUALITY

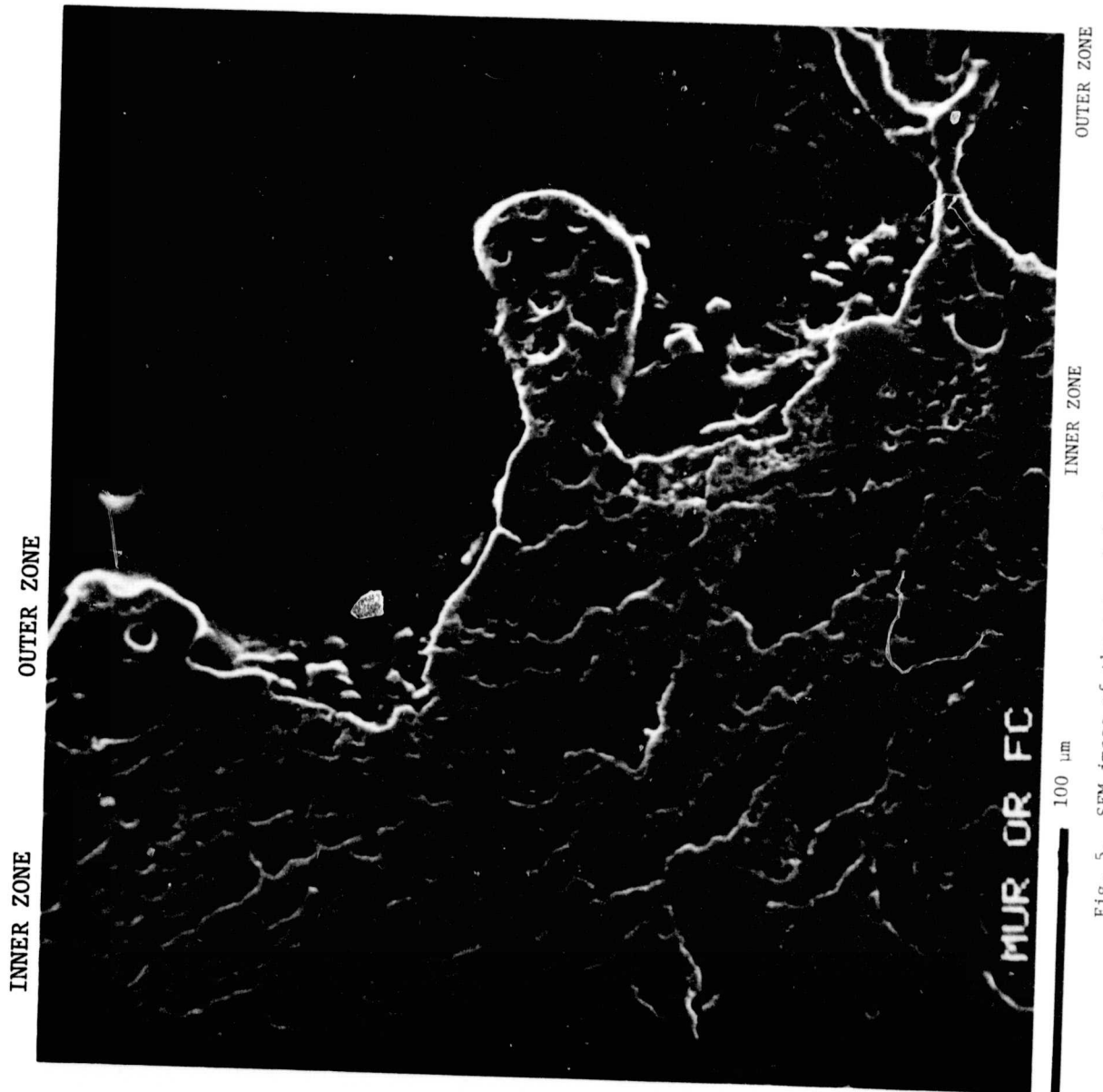


Fig. 5. SEM image of the natural fusion crust of the Murchison meteorite. The inner zone is characterized by voids and fractures through which vaporizing volatiles escape.

ORIGINAL PAGE IS
OF POOR QUALITY

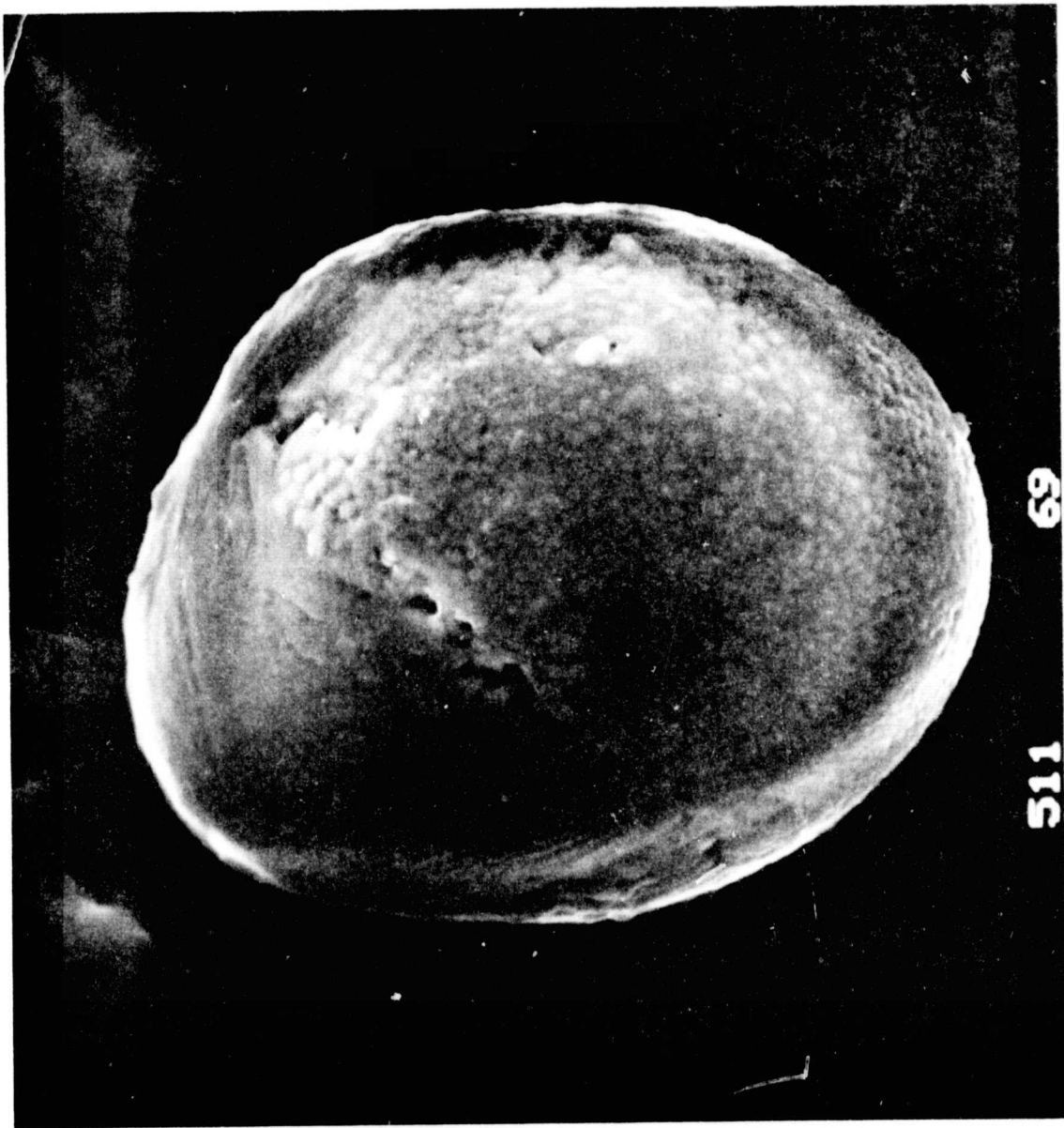
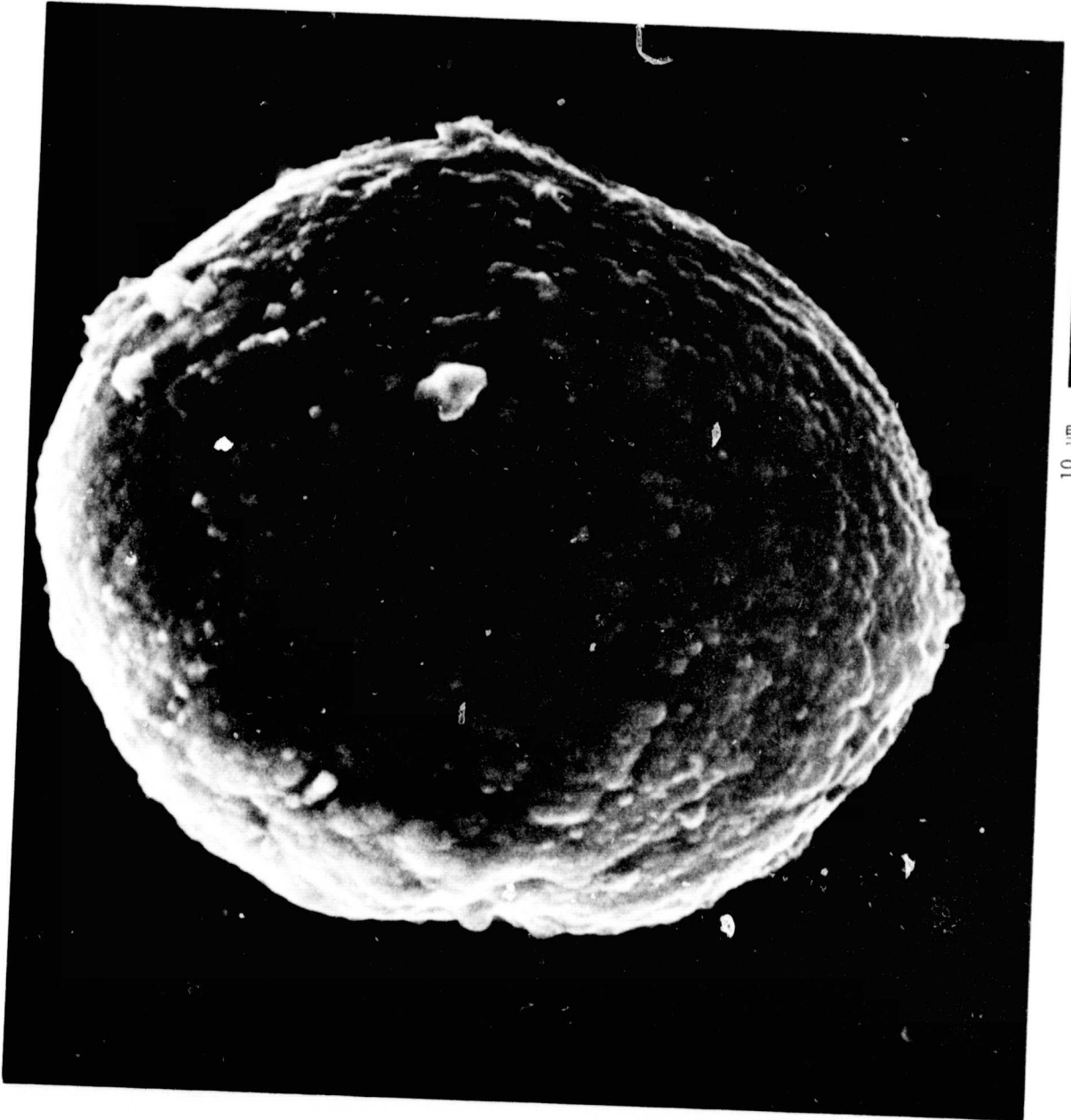


Fig. 6. SEM images of spherules ablated from the Murchison meteorite:
(a) silicate sphere composed of olivine, glass and magnetite (bright grains
at surface).

ORIGINAL PAGE IS
OF POOR QUALITY



10 μ m

Fig. 6. SEM images of spherules ablated from the Murchison meteorite:
(b) sulfide sphere composed of magnetite, pyrrhotite, and wustite.



Fig. 6. SEM images of spherules ablated from the Murchison meteorite:
(c) silicate spherule with an inclusion of the sulfide phase exposed at its
surface.

ORIGINAL PAGE IS
OF POOR QUALITY

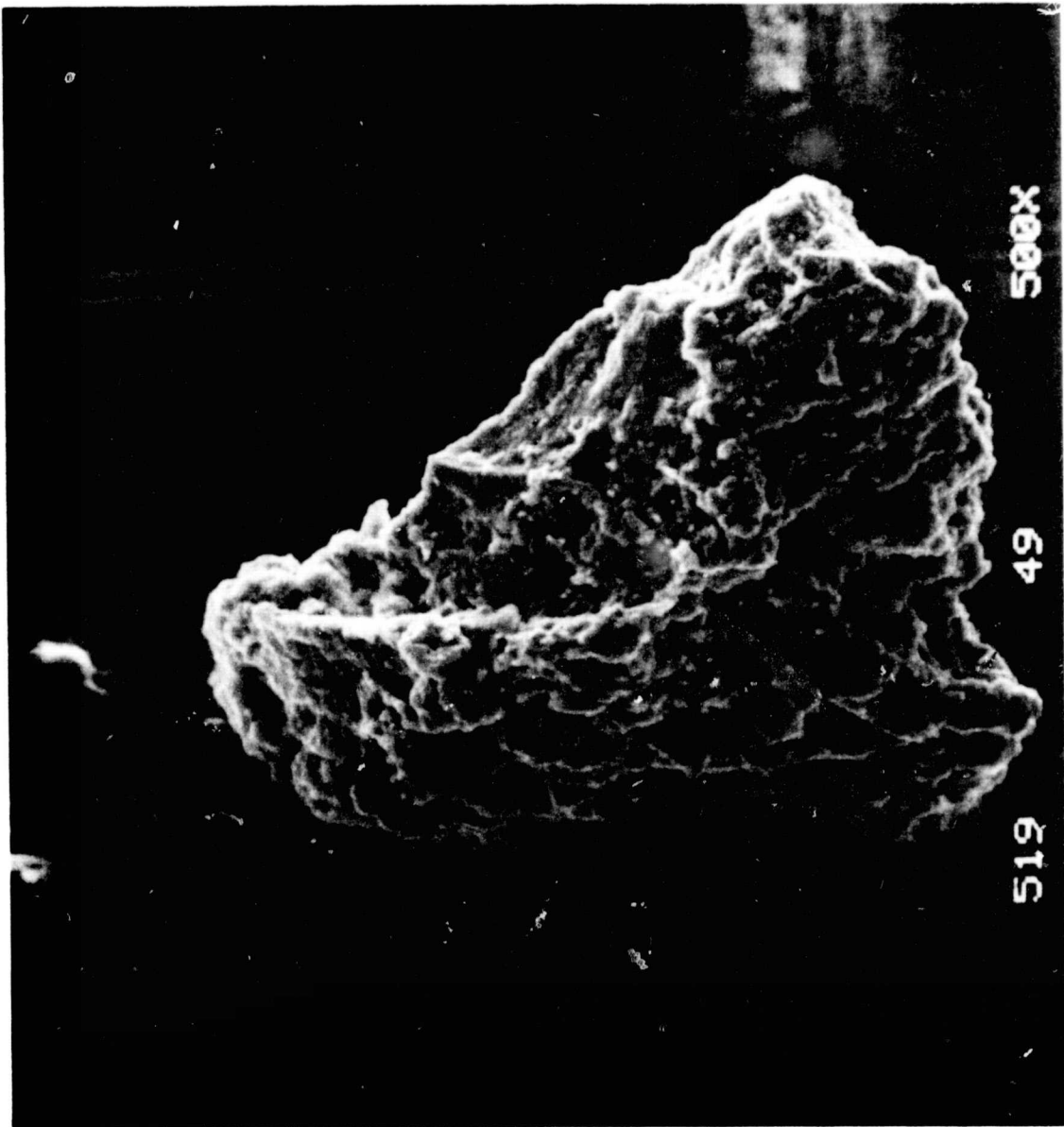


Fig. 7. SEM image of the most common type of fragmentary debris, a nonporous, fine-grained particle containing micron grains of olivine, magnetite, enstatite, and occasionally pyrrhotite.

ORIGINAL PAGE IS
OF POOR QUALITY

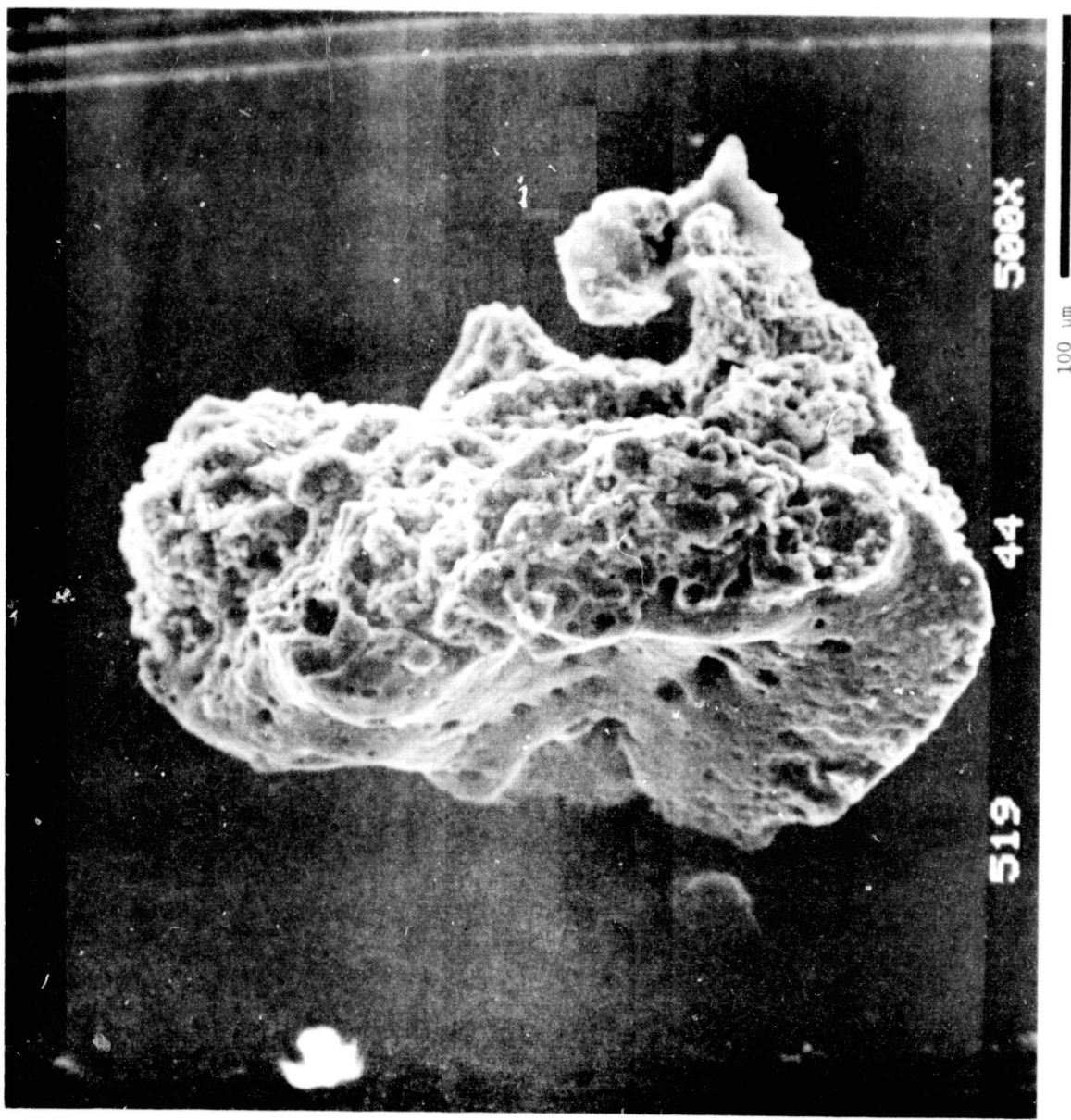
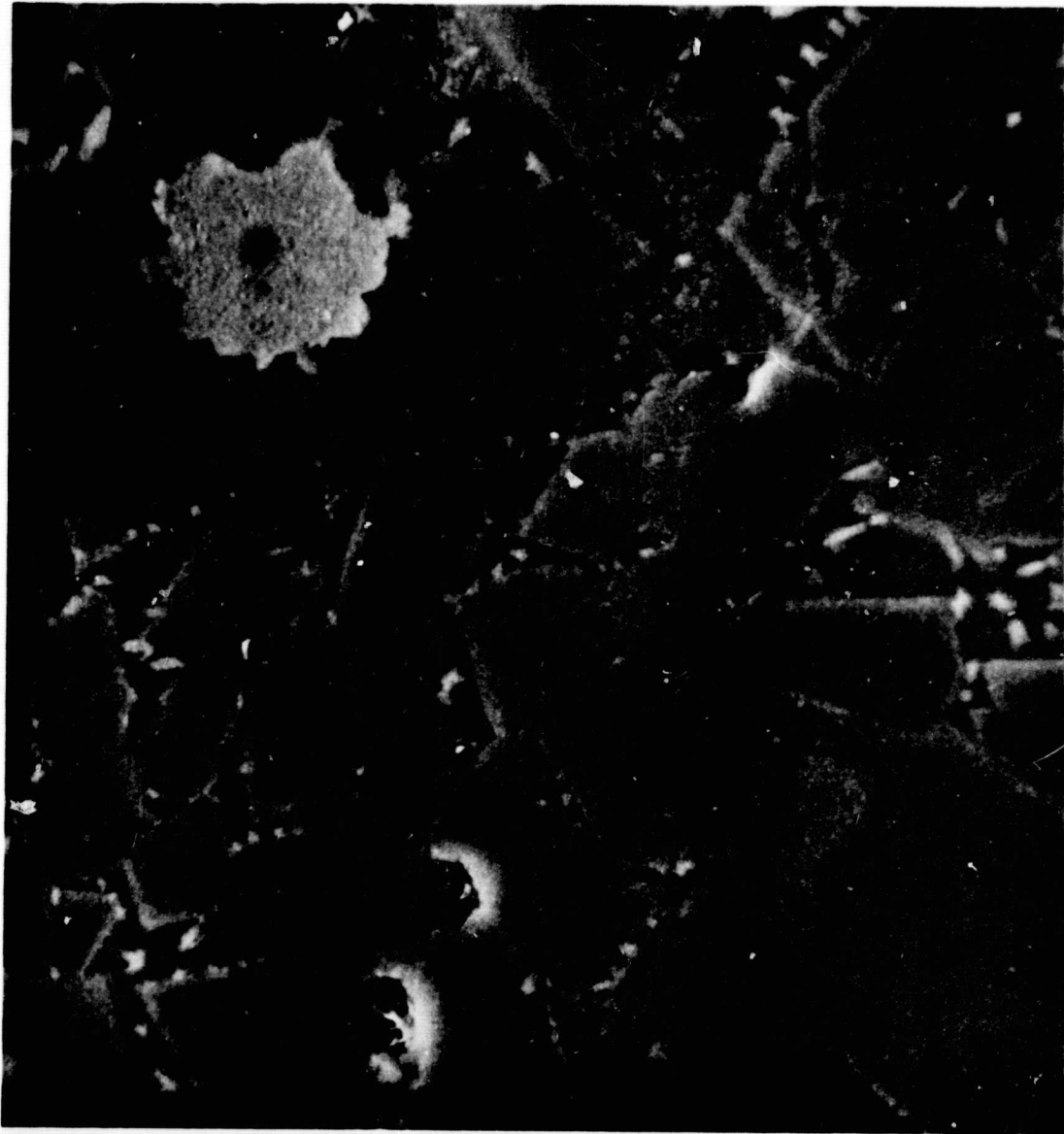


Fig. 8. SEM image of a fragmentary particle from the Murchison meteorite. Only one side of this particle shows evidence of melting, shown by a smooth fusion crust with numerous voids where volatiles have escaped.

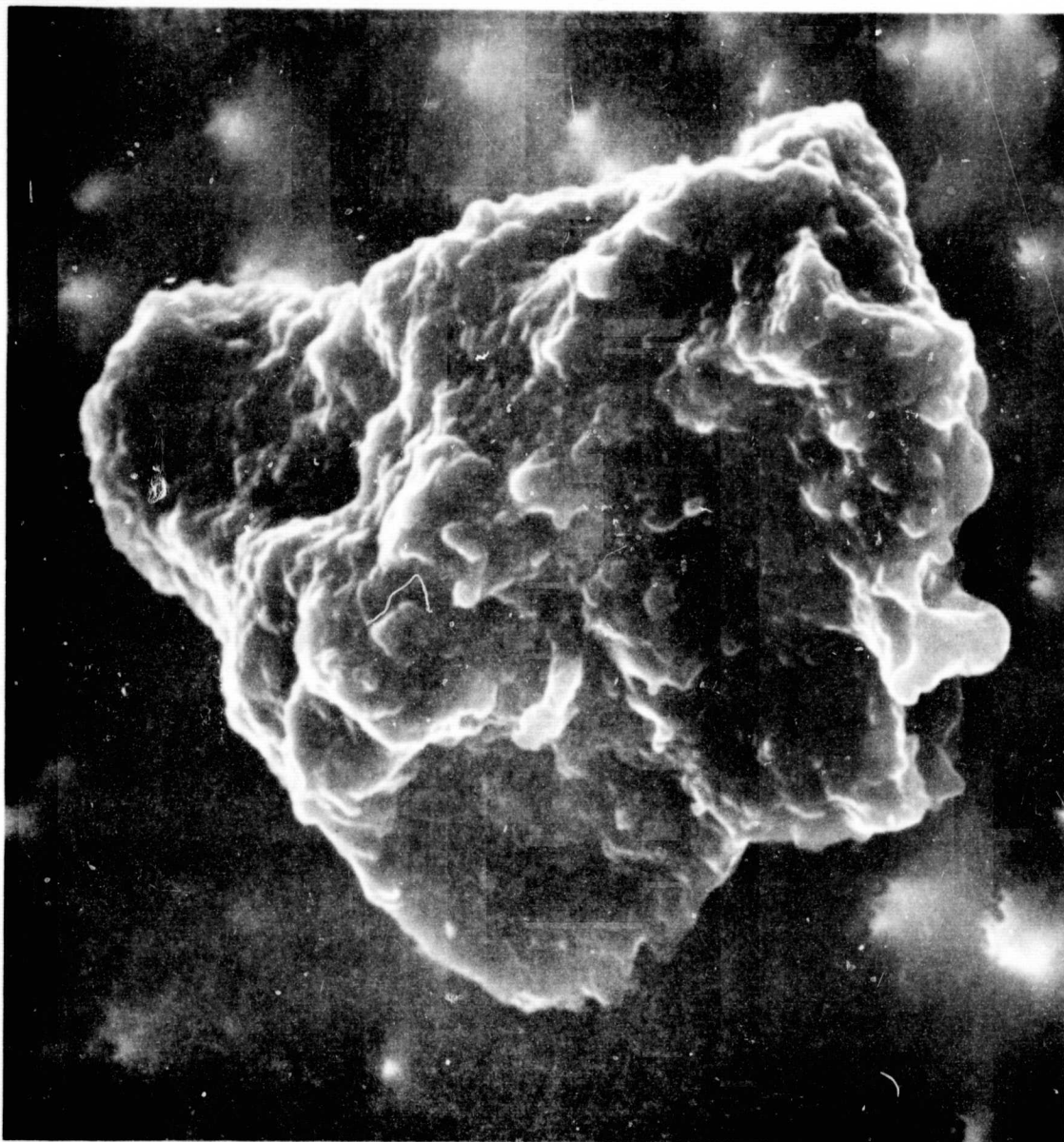
ORIGINAL PAGE IS
OF POOR QUALITY



10 μm

Fig. 9. SEM image of a polished section of a silicate spherule produced by artificial ablation of the Murchison meteorite. The large grey crystals are zoned olivine, the small bright crystals are magnetite, and the dark matrix is glass. The spherical inclusion is composed of iron sulfides but its outer rim has been altered to magnetite.

ORIGINAL PAGE IS
OF POOR QUALITY



10 μ m

Fig. 10. SEM image of a chondritic aggregate, nonporous particle from the U-2 stratospheric particle collection. Major elements are Si, Fe, Mg, S; minor elements are Ca, Al, Ni [Brownlee et al., 1976].

ORIGINAL PAGE IS
OF POOR QUALITY

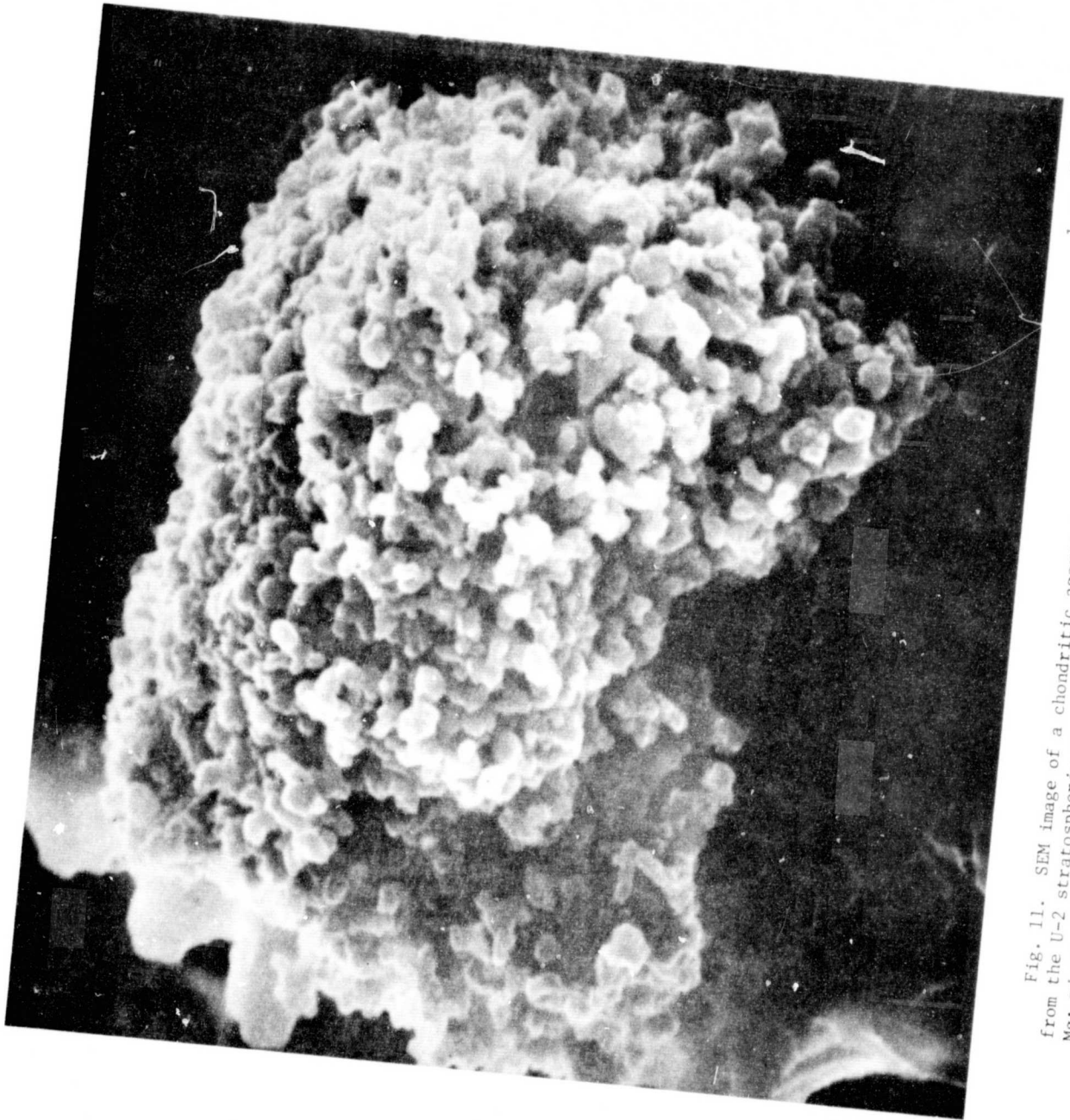


Fig. 11. SEM image of a chondritic aggregate, of unusually high porosity, from the U-2 stratospheric particle collection. Major elements are Si, Fe, S, Mg; minor elements are Ca, Ni, Al [Brownlee *et al.*, 1976].

ORIGINAL PAGE IS
OF POOR QUALITY

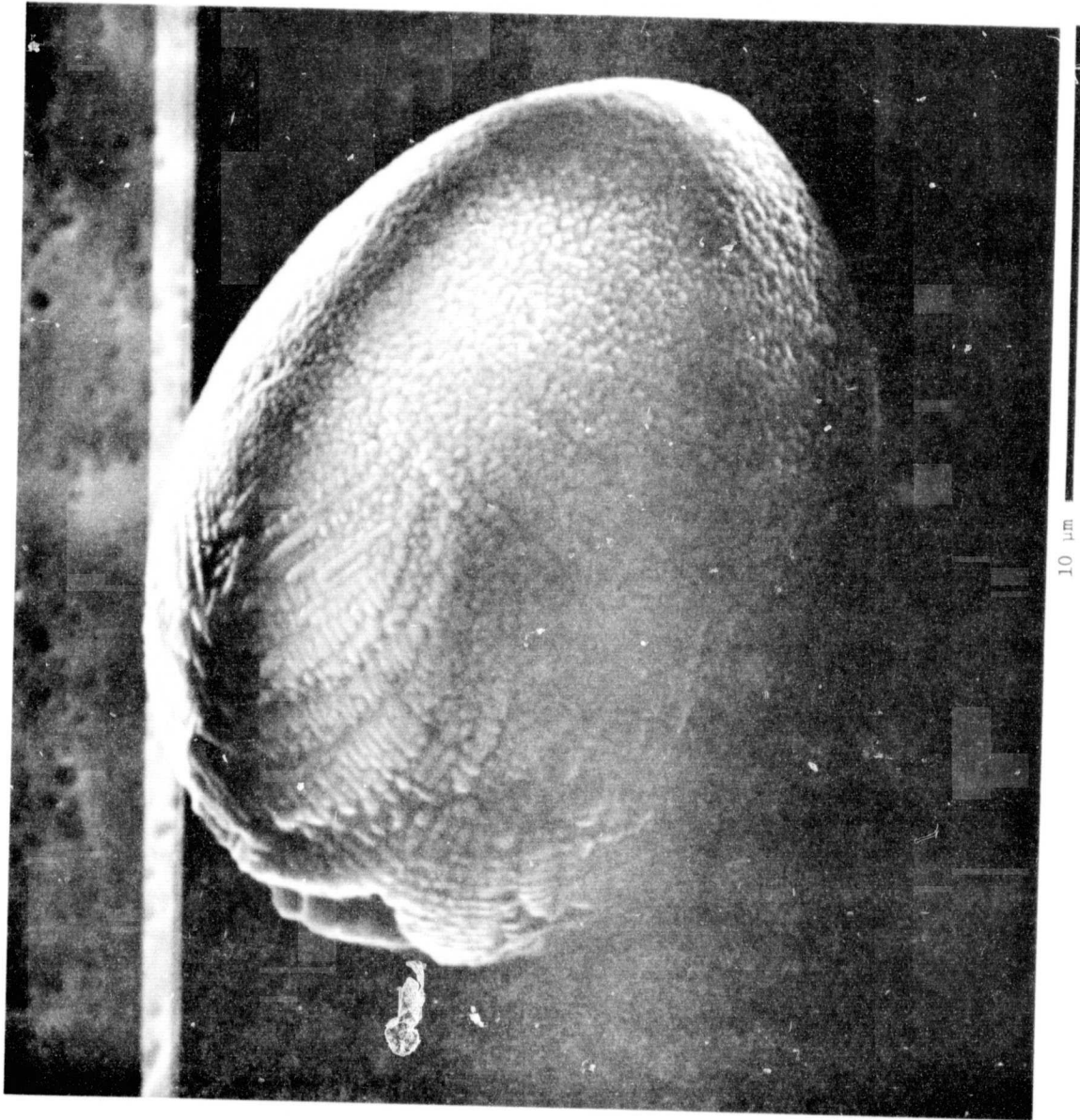


Fig. 12. SEM image of a chondritic ablation particle, spheroidal and showing submicron magnetite grains, from the U-2 stratospheric particle collection. Major elements are Fe, Si; minor elements are Mg, Ca, Al, Cr [Brownlee et al., 1976].

ORIGINAL PAGE IS
OF POOR QUALITY

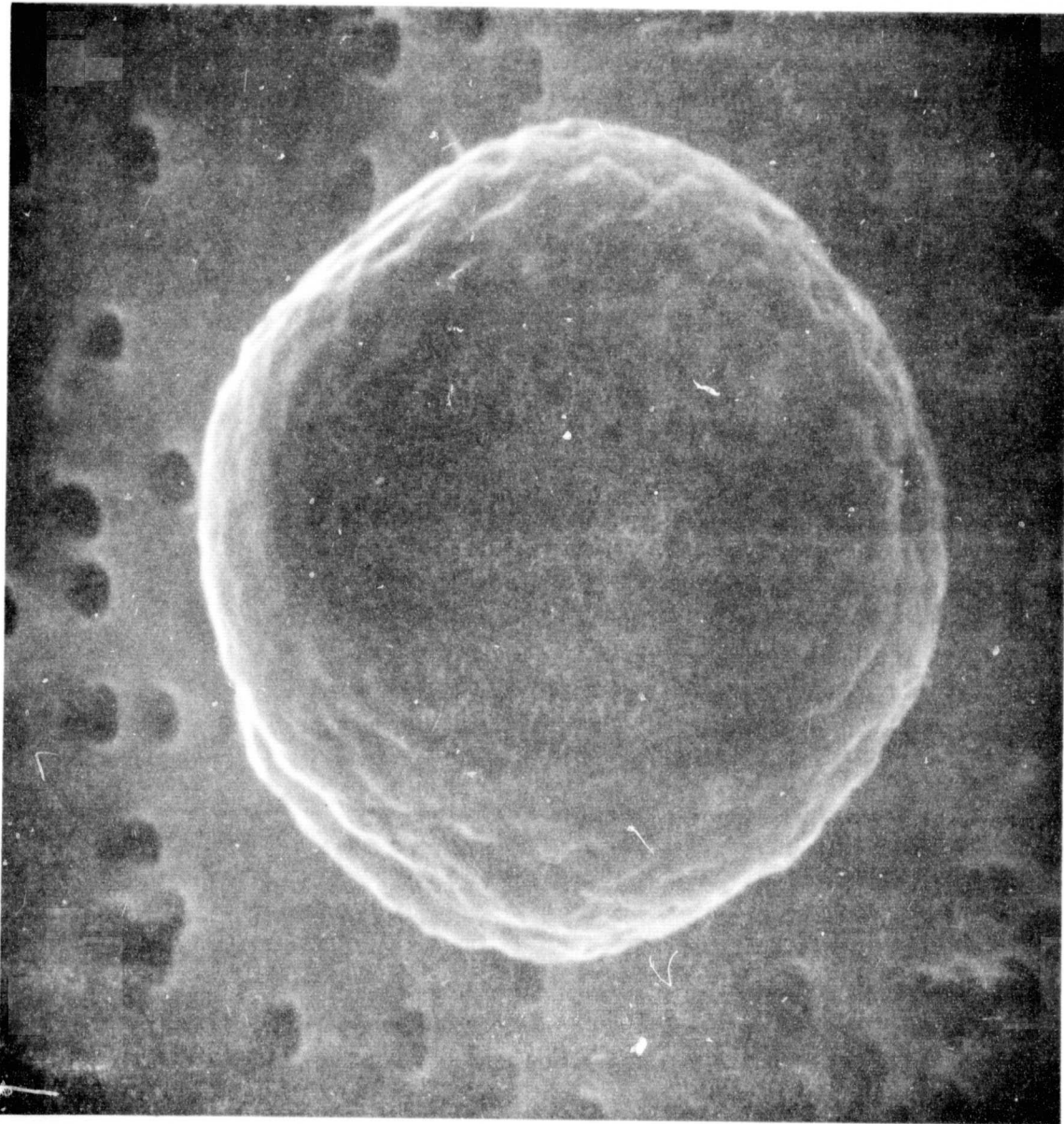


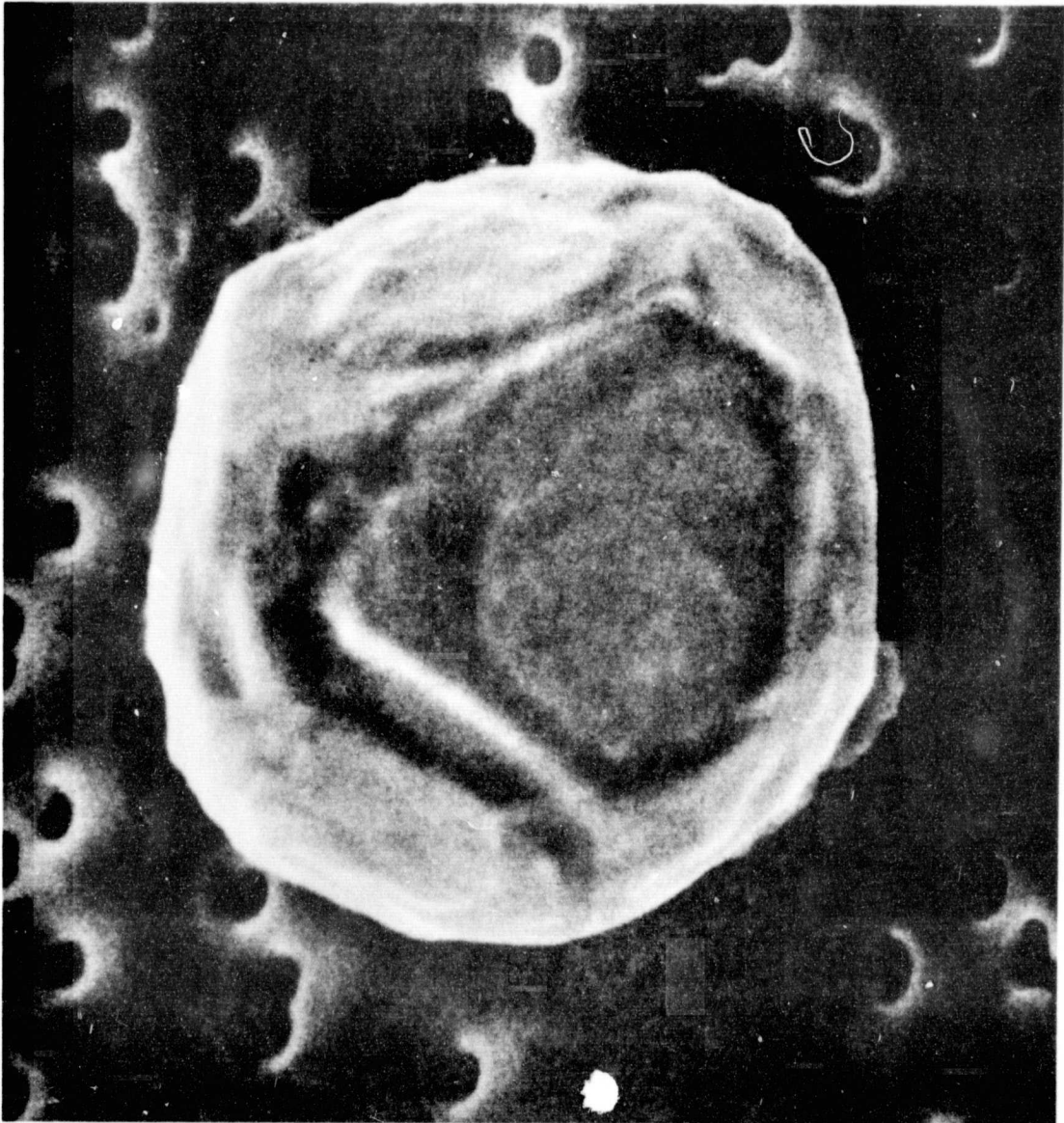
Fig. 13. SEM image of a FSN spherule from the U-2 stratospheric particle collection. Major elements are Fe, S; minor element is Ni [Brownlee et al., 1976].

ORIGINAL PAGE IS
OF POOR QUALITY



1 μm
Fig. 14. SEM image of an unusual FSN particle with platelet-like structure from the U-2 stratospheric particle collection [Brownlee et al., 1976].

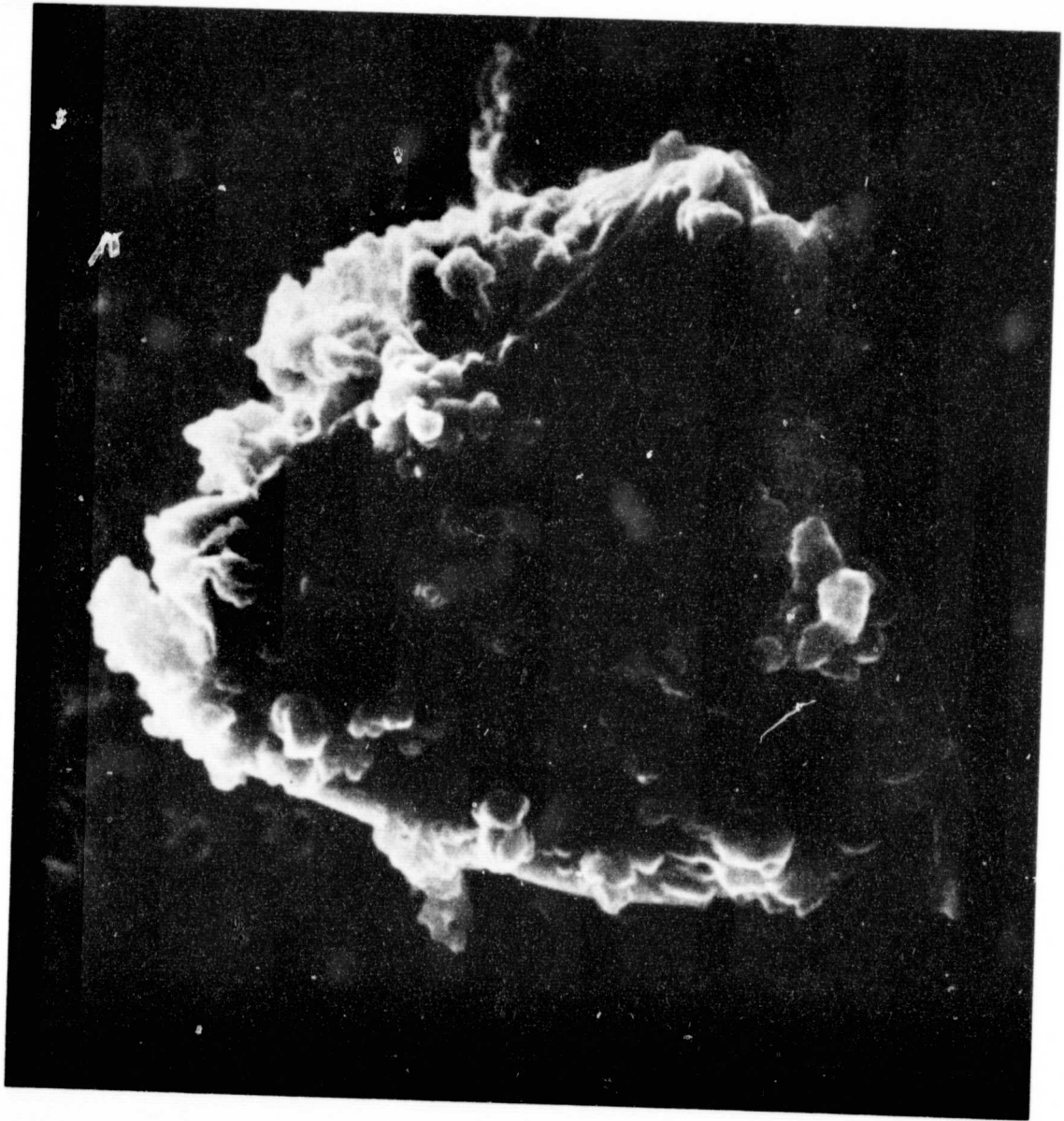
ORIGINAL PAGE IS
OF POOR QUALITY



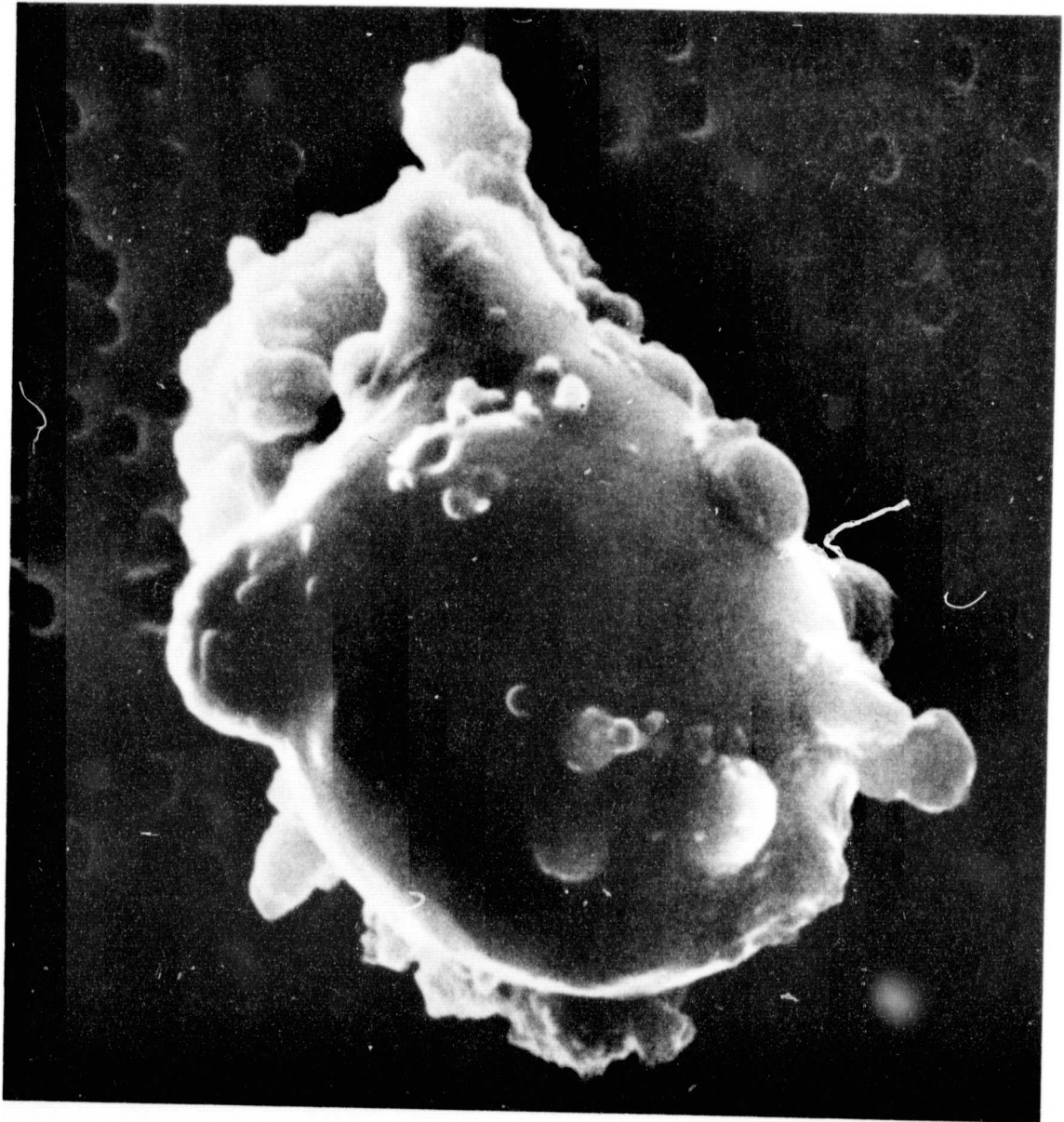
1 μm

Fig. 15. SEM image of an unusual FSN particle, with octahedron and cubic crystal faces, from the U-2 stratospheric particle collection. Major elements are Fe, S; minor element is Ni [Brownlee et al., 1976].

ORIGINAL PAGE IS
OF POOR QUALITY



1 μ m
Fig. 16. SEM image of a mafic silicate grain with adhering chondritic aggregate particles from the U-2 stratospheric particle collection. Mafic silicate major elements are Mg, Si; a minor element is Fe. Chondritic particle major elements are Si, Fe, Mg, S; minor elements are Ca, Al, Ni [Brownlee *et al.*, 1976].



1 μ m
Fig. 17. SEM image of an unusual round chondritic particle covered with Fe-Ni mounds. Major elements are Si, Mg, Fe; minor elements are Ca, Al, Ni, and Cr [Brownlee et al., 1976].